General Disclaimer

One or more of the Following Statements may affect this Document

- This document has been reproduced from the best copy furnished by the organizational source. It is being released in the interest of making available as much information as possible.

- This document may contain data, which exceeds the sheet parameters. It was furnished in this condition by the organizational source and is the best copy available.

- This document may contain tone-on-tone or color graphs, charts and/or pictures, which have been reproduced in black and white.

- This document is paginated as submitted by the original source.

- Portions of this document are not fully legible due to the historical nature of some of the material. However, it is the best reproduction available from the original submission.

NASA TECHNICAL MEMORANDUM

NASA TM-73700

NASA TM-73700

(NASA-TM-73700) FRACTURE SURFACE CHARACTERISTICS OF OFF-AXIS COMPOSITES (NASA) 23 p HC A02/MF A01 CSCL 11D

N78-13137

Unclas
G3/24 55228

FRACTURE SURFACE CHARACTERISTICS OF OFF-AXIS COMPOSITES

by J. H. Sinclair and C. C. Chamis
Lewis Research Center
Cleveland, Ohio 44135

TECHNICAL PAPER to be presented at the
Fourteenth Annual Meeting of the Society of Engineering Science, Inc.
Bethlehem, Pennsylvania, November 14-16, 1977

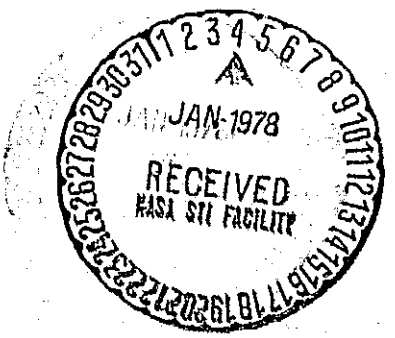

FRACTURE SURFACE CHARACTERISTICS OF OFF-AXIS COMPOSITES

J. H. Sinclair and C. C. Chamis

National Aeronautics and Space Administration
Lewis Research Center
Cleveland, Ohio 44135

E-9085-2

ABSTRACT

The fracture surface characteristics of off-axis high-modulus graphite-fiber/epoxy composite specimens were studied using a scanning electron microscope (SEM). The specimens were subjected to tensile loading at various angles (0° - 90°) to the fiber direction. SEM photomicrographs of the fractured surfaces revealed three different load angle regions with distinct fracture characteristics. Based on these revelations, criteria were established which can be used to characterize fracture surfaces with respect to a predominant "single-stress" fracture mode.

INTRODUCTION

Off-axis tensile data for unidirectional composites are of considerable interest to the fiber composite community for several important reasons. Some of these are: (1) determination of the variation of elastic properties and fracture stress (strain) as a function of load angle (angle between fiber and load directions), (2) verification of composite macromechanics theories for elastic properties and for combined-stress fracture, and (3) generation of fundamental information for assessing angleplied laminate mechanical behavior.

An investigation of the first two aspects dealing with boron-fiber/epoxy composites is reported in [1]. A brief review of previous work is also covered in this reference. However, the third aspect has not

been examined with respect to fracture modes, morphology of fracture surfaces, and criteria for identifying these fracture modes.

The objective of this investigation was to study the surface morphology of fractured specimens made from unidirectional high-modulus graphite-fiber composites and subjected to off-axis tensile load. The focus of the investigation was on identifying distinct features of fracture surfaces using the scanning electric microscope and on establishing criteria to characterize these fracture surfaces. A broader scope of the investigation from which this was a part is described in a forthcoming NASA TN publication now being prepared.

SPECIMEN PREPARATION, TESTING, AND EXAMINATION

The laminate consisted of eight unidirectional plies of Modmor-I graphite fibers in a matrix of ERLA-4617 epoxy resin cured with meta-phenylene di-amine (MPDA). Tensile specimens were cut from the laminate plate at the desired load angles and dressed down to the required 0.500 inch width by diamond wheels. Specimen ends were reinforced with adhesively bonded fiber glass tabs. The tensile specimens were then instrumented with strain gages. Figure 1 shows a completed specimen; a schematic of specimen geometry and strain gage arrangement is shown in figure 2. The test specimens were placed in the grips pictured in figure 3 and loaded to fracture using a hydraulically actuated universal testing machine. Loading was incremental to facilitate periodic recording of strain gage data.

Fractured surfaces from each tensile specimen shown in figure 4 were observed by scanning electron microscope, and typical photomicrographs were made to illustrate fracture modes.

Segments of tested laminates containing the fracture surfaces of interest were cut (while carefully preserving fracture surfaces) from each specimen and cemented (on edge with fracture surface up) to aluminum mounts. In order to facilitate observation using the SEM, the

specimens were made electrically conductive by coating them with a gold-palladium film approximately 200 angstron units (2×10^{-6} cm) thick which was applied by vapor deposition in a vacuum evaporator. They were then studied and photographed with a JUL-JSM-2 scanning electron microscope.

RESULTS

The results of tensile testing and of the SEM studies are discussed in this section

Tensile Test Results

A summary of some of the tensile properties determined during this study is presented in table I. The specimens tested along the fiber direction broke at 81.7 ksi and the fracture strengths of the specimens decreased gradually with increasing load angle; the transverse specimen (90° off-axis) broke at 4 ksi. The moduli decreased in a similar manner with increasing load angle and lie between almost 35 million psi for the longitudinal specimen (0° off-axis) and just over 1 million psi for the 90° off-axis specimen. Stress strain curves for the specimens tested at the various angles are presented in figure 5. Note that they are all linear to fracture.

S.E.M. Study Results

The fractured surfaces of the specimens were examined using a scanning electron microscope (SEM) for the purpose of identifying regions of distinct or predominant fracture modes associated with the different load angles. SEM photomicrographs of all the specimens tested are presented in figures 6 to 14 at three different magnifications.

The fracture surface of the 0° specimen is shown in figure 6. As can be observed, in figure 6(a) the fracture surface is irregular. An area replete with pulled-out fibers that broke off at varying lengths can be observed in the left foreground of figure 6(a). This type of

fracture suggests poor bonding between matrix and fibers. The remaining areas of figure 6(a) show irregularly shaped tiered or stepped surfaces that are typical of the fracture surface of specimens tested in longitudinal tension. At some regions, fibers over relatively large areas fractured at approximately the same level, and they show little fiber pull-out. This is the type of fracture surface shown in figures 6(b) and (c). There was strong bonding between the fibers and matrix in these areas. The fracture mode of the resin was cleavage (fig. 6(c)). Lateral fiber surfaces of these stepped zones show some evidence of sheared resin lying between the fibers as seen in the upper left of figure 6(c).

The fracture surface in figure 6(c) reveals several distinct features. These features and some significant implications following therefrom are as follows:

1. The fiber fracture surface is irregular but appears to be symmetric from the perimeter towards the center. This type of fiber fracture surface morphology will be considered to be typical of tensile fracture.

2. The matrix fracture surface between fibers at the same level is smooth indicating tensile brittle fracture by cleavage.

3. The matrix fracture surface between fibers at different levels is lacerated indicating fracture by tear which will be considered to "fracture by intralaminar shear."

4. The surface of fibers that pulled-out appears to be clear of matrix residue, in general. This indicates weak interfacial bonding which may be construed to imply that "the interfacial bond is predominantly mechanical."

5. The transverse split in the left foreground is probably caused by the elastic energy release after fracture "back-lash."

The fracture surface of the 5° off-axis tensile specimen, figure 7, reveals the following features:

1. Surface tiering (fig. 7(b)) and matrix cleavage (fig. 7(c)) both of which are indicative of tensile fracture.

2. Extensive matrix surface lacerations indicating substantial fracture by intralaminar shear.

3. Fiber pull-out and surfaces free of matrix residue indicating weak interfacial bonding. Recall that all of the above features were observed in the fracture surface of the 0° tensile specimen.

The fracture of the 10° off-axis tensile specimen of figure 8 reveals: (1) matrix surface lacerations and (2) fiber surfaces free of matrix residue. Both of these features indicate that the intralaminar shear fracture mode became dominant between the 5° and 10° off-axis loadings. We will consider this angle range to fracture by intralaminar shear stress. This observation as well as certain theoretical considerations not covered herein led to the recommendation that: "The 10° off-axis tensile specimen is suitable for intralaminar shear characterization of unidirectional fiber composites [2]."

The fracture surfaces of the 15° and 30° off-axis tensile specimens figures 9 and 10 reveal similar features to those of the 10° off-axis tensile specimen. These surfaces, too, indicate that fracture was induced mainly by intralaminar shear stress.

The fracture surface of the 45° off-axis, figure 11, tensile specimen reveals the following features:

1. Matrix cleavage with irregular boundary indicating some transverse tensile fracture.

2. Matrix debris resulting probably from tensile matrix fracture.

3. Some matrix lacerations indicating some intralaminar shear stress fracture interaction.

The above surface fracture features show that another fracture mode becomes active somewhere between a load angle of 30° and 45°. This mode will be construed to be induced by the transverse tensile stress.

The fracture surfaces of the 60° off-axis tensile specimen, figure 12, and the 75°, figure 13, reveal mainly matrix cleavage and some fiber surface free of matrix residue; both of these features indicate that fracture was induced by transverse tensile stress.

The fracture surface of the 90° tensile specimen, figure 14, reveals the following features:

1. Matrix cleavage indicative of tensile fracture of brittle materials

2. Fiber surfaces free of matrix residue indicative of weak interfacial bond as was already mentioned.

The above features indicate that transverse tensile stress produces fracture surfaces characterized by: (1) matrix cleavage and (2) fiber surfaces clear of matrix residue.

The above discussion leads to the following criteria for studying and classifying fracture and fracture surfaces in MOD I - graphite fiber/resin matrix composites.

1. Fiber tensile fracture - The surface morphology is tiered and is characterized by the following:

a. irregular fiber surface with some symmetry from the perimeter inward

b. matrix cleavage surface

c. fiber pull-out with fiber surfaces clear of matrix residue

d. some matrix lacerations on inter-fiber surfaces connecting two different tier levels

e. fiber fracture appears to occur at load angles near 0° and possibly up to 5°.

2. Intralaminar shear stress fracture - the fracture surface produced by this stress is mainly level or plane and is characterized by the following:

a. extensive matrix lacerations

b. fiber surfaces free of matrix residue

c. intralaminar shear stress appears to induce fracture at the load angle (θ) range $5° < \theta < 30°$ and contributes significantly to fracture in the load angle (θ) range somewhere between 15° and 30° to 45°.

3. Transverse tensile stress fracture - The fracture surface produced by this stress is level and is characterized by the following:

a. matrix cleavage

b. fiber surfaces free of matrix residue

c. some matrix debris

d. transverse tensile stress appears to induce fracture in the load angle (θ) range $45° \leq \theta \leq 90°$ and contributes significantly to fracture in the load angle (θ) range somewhere between 15° and 30° to 45°.

4. Mixed mode fracture - The fracture surface produced by mixed mode is regular and is characterized by a mixture of lacerated and cleavaged surfaces which are produced by combinations of intralaminar shear and transverse tensile fracture. This mode is prevalent in the load angle range (θ) between 15° and 30° to 45°.

The four criteria stated above and the physical characteristics associated with them have not been reported previously to the authors' knowledge. These should provide researchers with a set of definite guidelines for identifying and classifying fracture in graphite-fiber/resin-matrix composites. And, since the matrix appears to dominate fracture in the load angle (θ) range $5° < \theta \leq 90°$ via either intralaminar shear or transverse tensile, the above criteria should be applicable to all fiber/resin-matrix composites.

SUMMARY OF RESULTS AND CONCLUSIONS

The major results and conclusions of an investigation to study the fracture surface characteristics of fiber composites subjected to off-axis tensile loadings by examination with a scanning electron microscope are:

1. Fracture surfaces of off-axis tensile specimens exhibit distinct morphological characteristics:

a. Irregular with fiber pull-out near load angle of 0° to the fiber direction.

b. Extensive amount of matrix lacerations in the load angle range $5° < \theta < 30°$.

c. Matrix cleavage in the load angle range $45° \leq \theta \leq 90°$.

d. Mixed mode lacerations and cleavage between 15° to 30° and 45°.

2. Criteria were established for characterizing fracture surfaces and identifying the associated loading angle in off-axis tensile specimens;

a. Longitudinal tensile stress fracture - irregular fracture surface with fiber pull-out, $0° \leq \theta < 5°$.

b. Intralaminar shear stress fracture - regular fracture surface with extensive matrix lacerations, $5° < \theta < 30°$.

c. Transverse tensile stress fracture - regular fracture surface with extensive matrix cleavage, $45° \leq \theta \leq 90°$.

d. Mixed mode fracture - regular surface with lacerations and cleavage between 15° and 30° to 45°.

3. The results of this investigation should provide a good foundation for identifying, characterizing and quantifying fracture modes in off-axis and angleplied laminates.

REFERENCES

1. R. S. Sandu, "Nonlinear Behavior of Unidirectional and Angle Ply Laminates," J. Aircraft, 13, 104-111 (1976).

2. C. C. Chamis and J. H. Sinclair, "10° Off-Axis Tensile Test for Intralaminar Shear Characterization of Fiber Composites," NASA TN D-8215 (1976).

TABLE I. - SUMMARY OF MEASURED TENSILE DATA (MODMOR I/EPOXY SPECIMENS)

Specimen	Load angle, deg	Specimen[a] thickness, in.	Fracture load, lb	Fracture stress, ksi	Fracture strain, ε_{xx}, percent	Modulus, psi
A-0	0	0.053	2152	81.7	0.231	34.9×10^6
A-5	5	.056	1540	55.2	.188	29.3
A-10	10	.056	1390	49.8	.286	17.8
A-15	15	.056	798	28.7	.284	10.4
A-30	30	.057	357	12.7	.365	3.49
A-45	45	.056	210	7.5	.390	1.97
A-60	60	.056	160	5.7	.413	1.31
A-75	75	.057	128	4.5	.385	1.20
A-90	90	.052	104	4.0	.364	1.12

[a]Nominal spec. width = 0.500 inch.

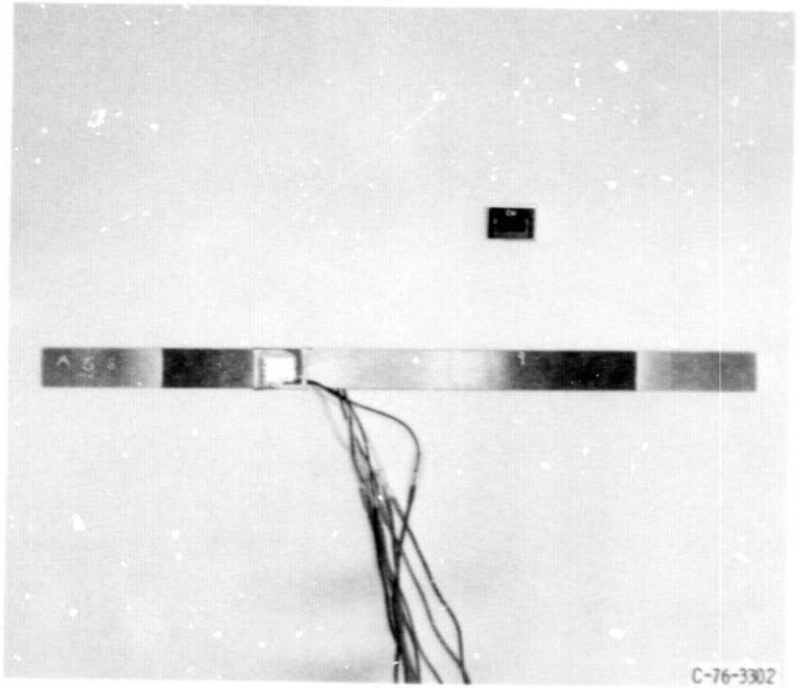

Figure 1. - Untested tensile specimen.

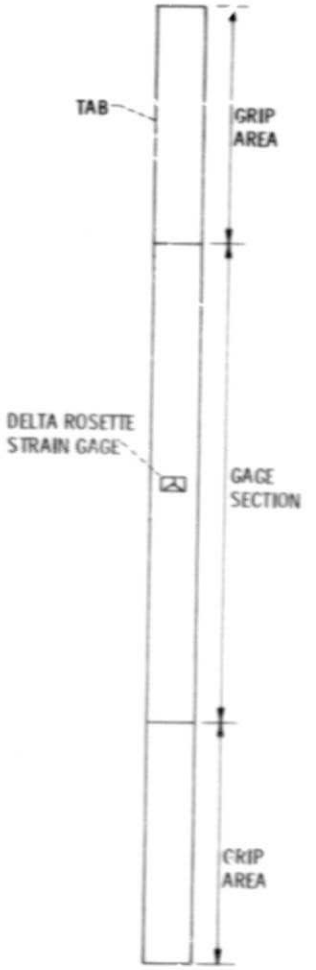

Figure 2. - Schematic of specimen geometry and strain gage arrangement.

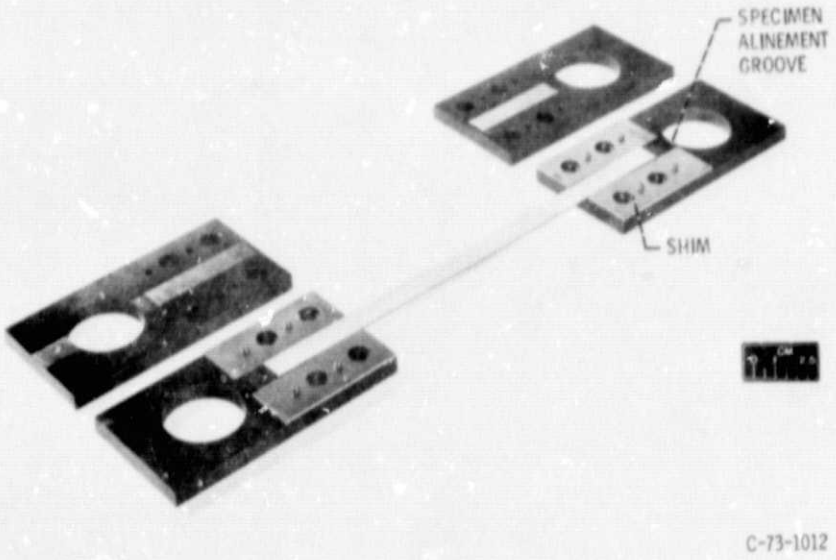

Figure 3. - Grips for composite tensile specimens.

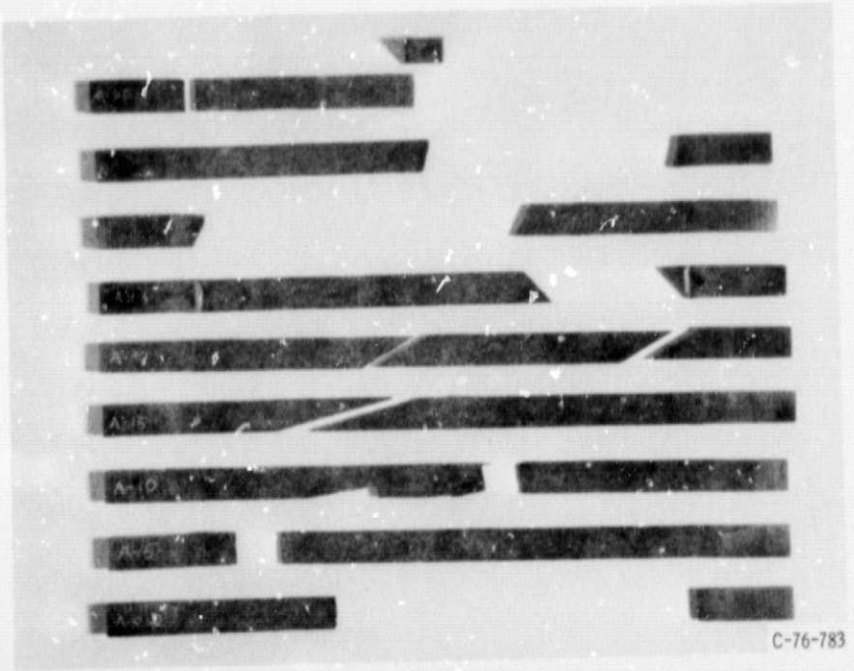

Figure 4. - Fractured tensile specimens.

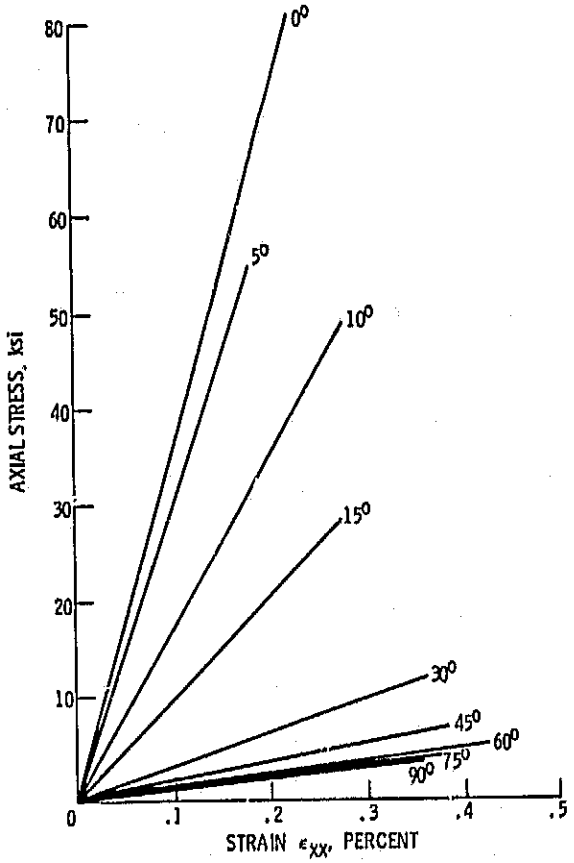

Figure 5. - Stress-strain curves for specimens subjected to tensile loading at various angles.

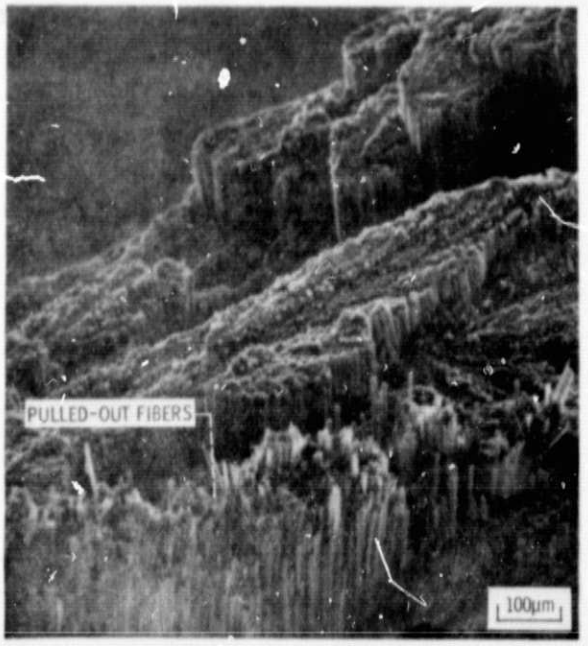

(a) GENERAL VIEW

(b) DETAILED VIEW

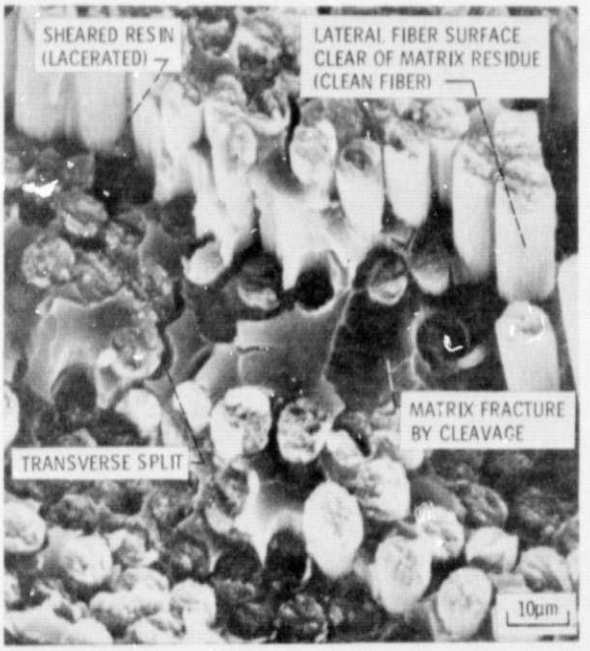

(c) ENLARGEMENT OF DETAIL IN (b) TO SHOW FRACTURE MODE.

Figure 6. - Scanning electron photomicrographs of fractured surface of MOD I/Epoxy composite $[0]_8$ tested parallel to the fiber direction.

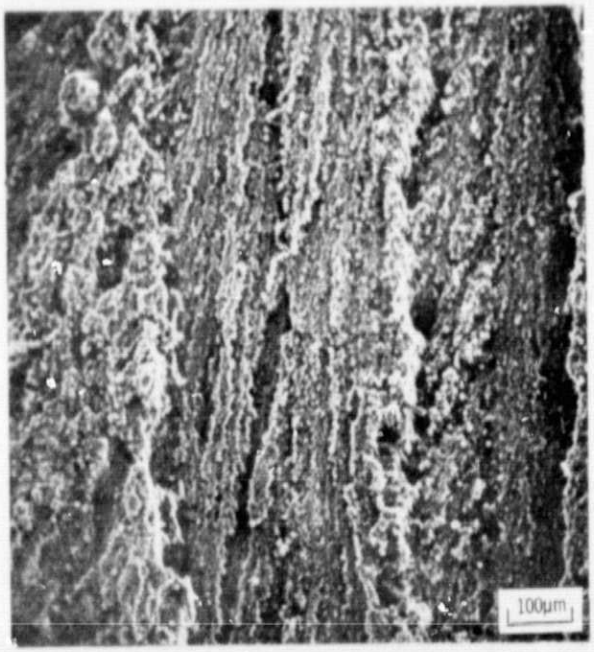

(a) GENERAL VIEW

(b) DETAILED VIEW

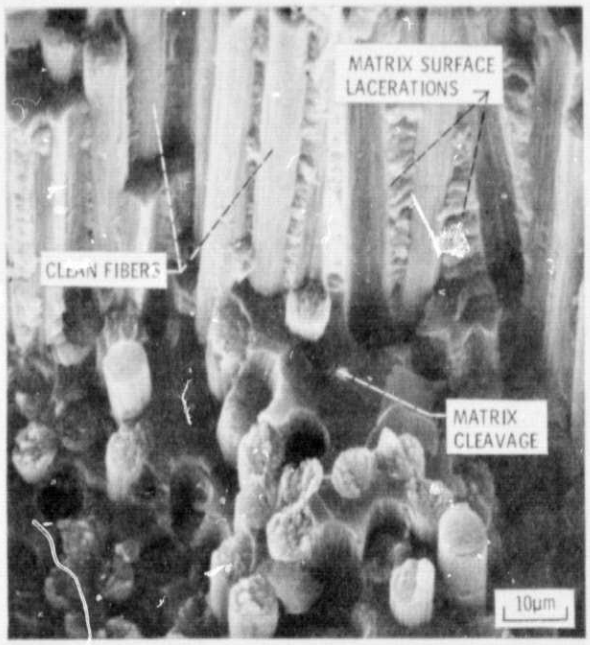

(c) ENLARGEMENT OF DETAIL IN (b) TO SHOW FRACTURE MODE

Figure 7. - Scanning electron photomicrographs of fractured surface of MOD I/Epoxy composite $[0]_8$ tested at 5 degrees to the fiber direction.

(a) GENERAL VIEW

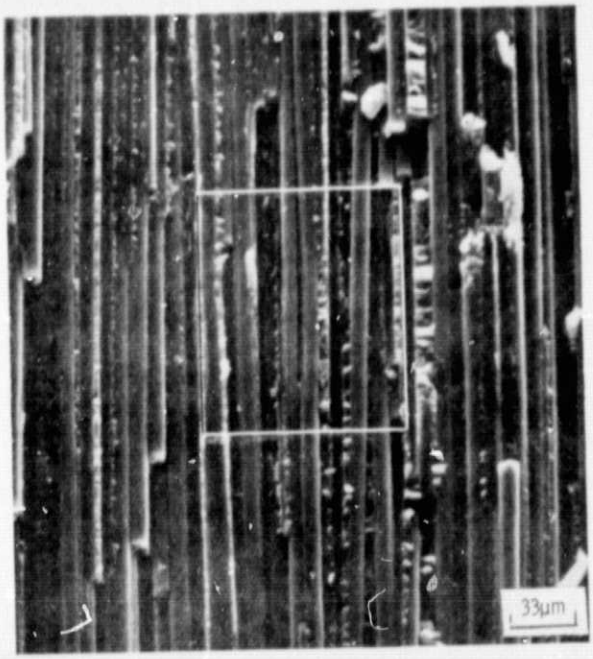

(b) DETAILED VIEW

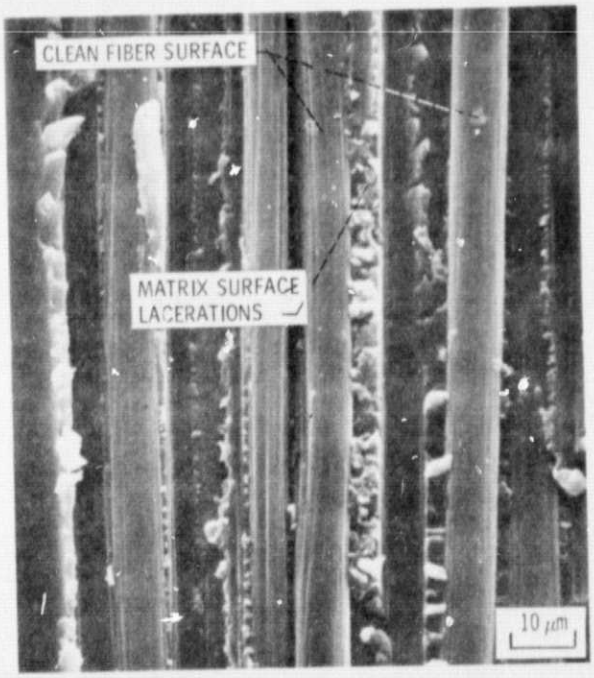

(c) ENLARGEMENT OF DETAIL IN (b) TO SHOW FRACTURE MODE.

Figure 8. - Scanning electron photomicrographs of fractured surface of MOD I/Epoxy composite $[0]_8$ tested at 10 degrees to the fiber direction.

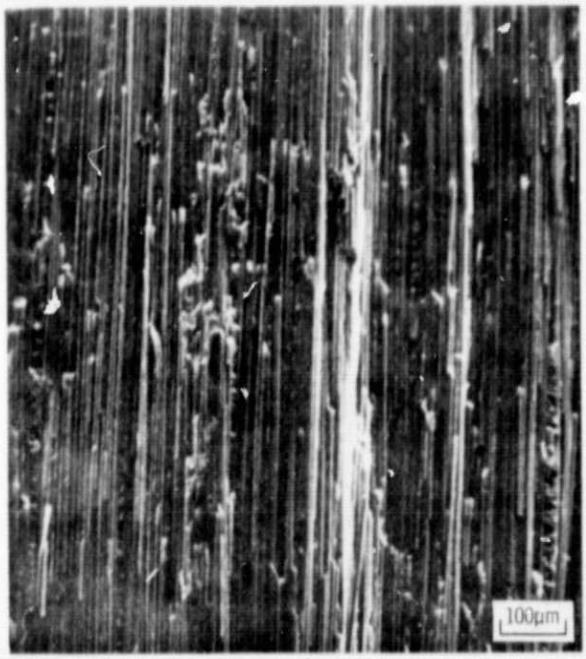

(a) GENERAL VIEW

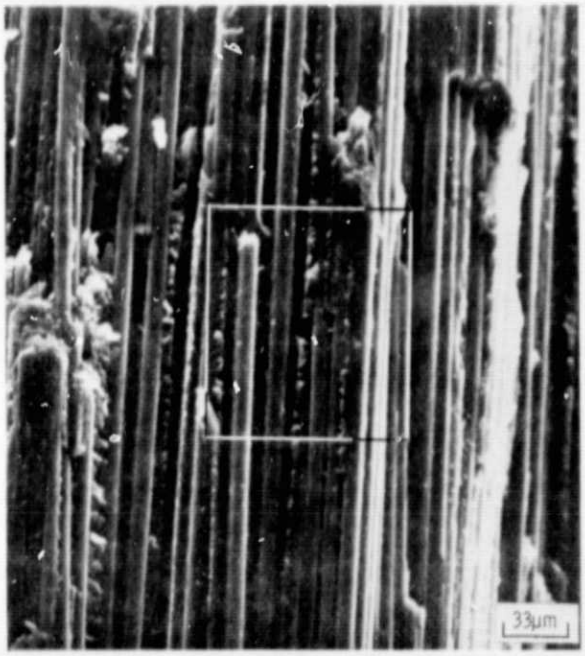

(b) DETAILED VIEW

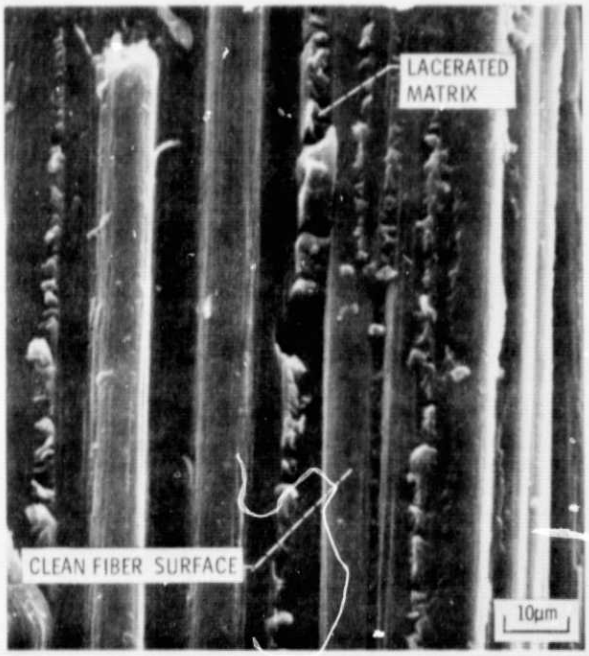

(c) ENLARGEMENT OF DETAIL IN (b) TO SHOW FRACTURE MODE.

Figure 9. - Scanning electron photomicrographs of fractured surface of MOD I/Epoxy composite $[0]_8$ tested at 15 degrees to the fiber direction.

(a) GENERAL VIEW

(b) DETAILED VIEW

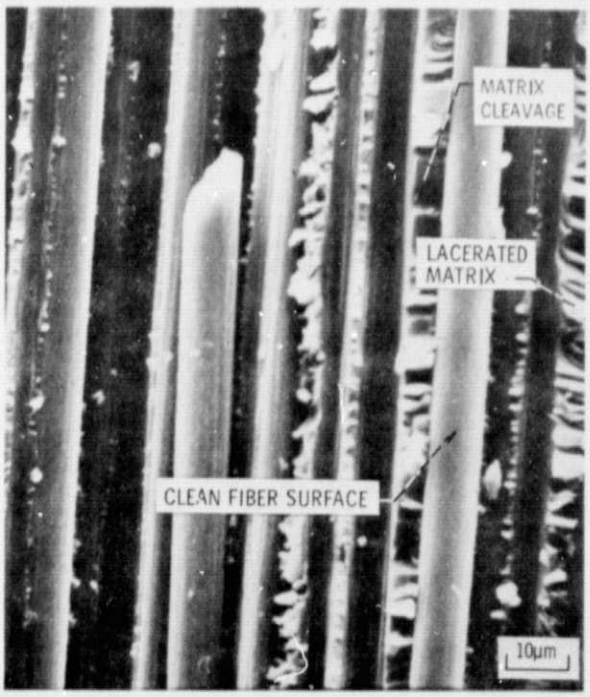

(c) ENLARGEMENT OF DETAIL IN (b) TO SHOW FRACTURE MODE.

Figure 10. - Scanning electron photomicrographs of fractured surface of MOD I/Epoxy composite $[0]_8$ tested at 30 degrees to the fiber direction.

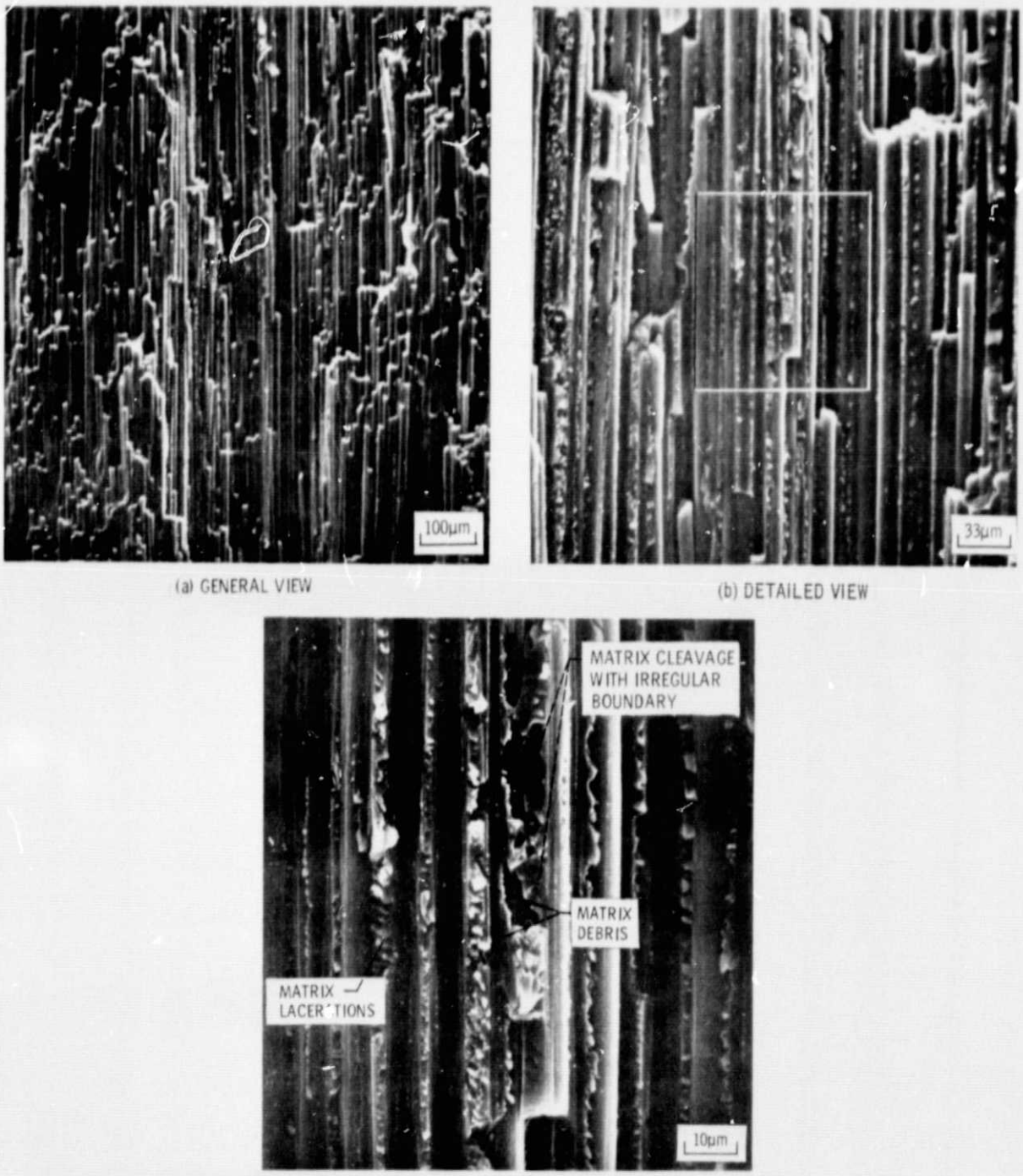

(a) GENERAL VIEW

(b) DETAILED VIEW

(c) ENLARGEMENT OF DETAIL IN (b) TO SHOW FRACTURE MODE.

Figure 11. - Scanning electron photomicrographs of fractured surface of MOD I/Epoxy composite $[0]_8$ tested at 45 degrees to the fiber direction.

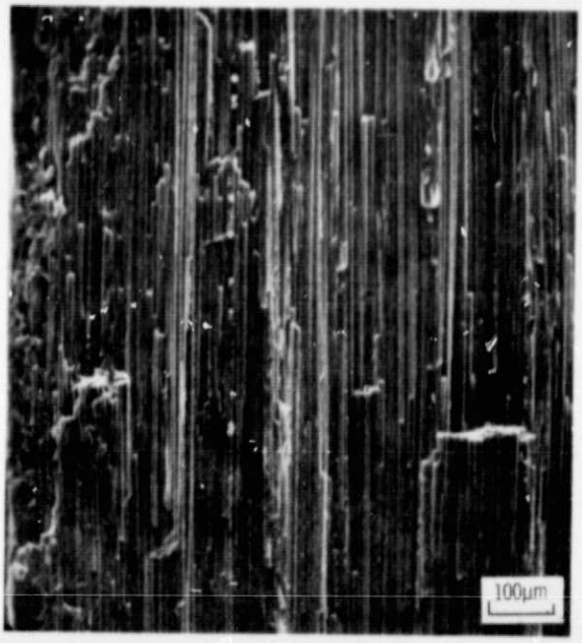

(a) GENERAL VIEW

(b) DETAILED VIEW

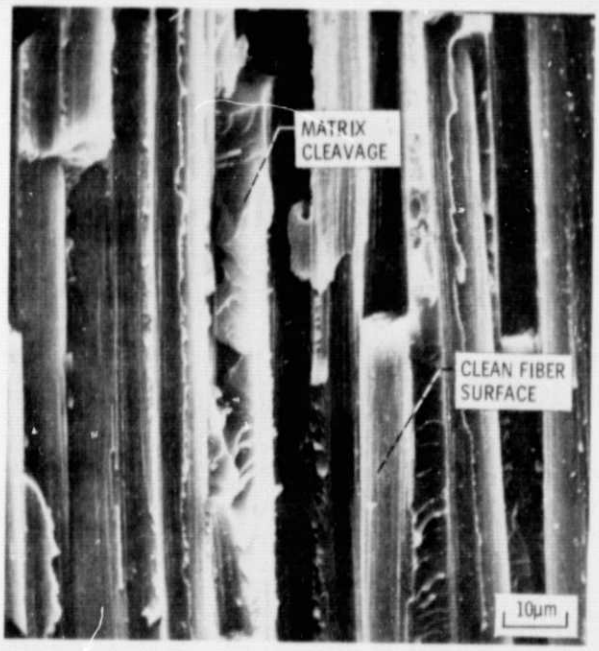

(c) ENLARGEMENT OF DETAIL IN (b) TO SHOW FRACTURE MODE.

Figure 12. - Scanning electron photomicrographs of fractured surface of MOD I/Epoxy composite $[0]_8$ tested at 60 degrees to the fiber direction.

(a) GENERAL VIEW

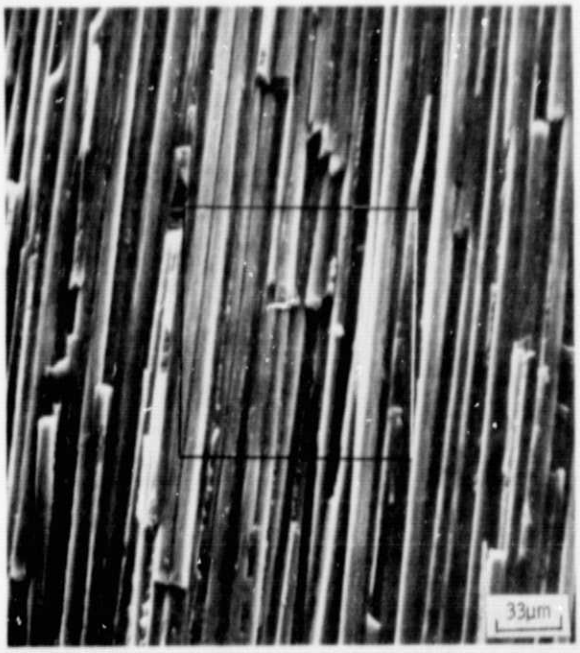

(b) DETAILED VIEW

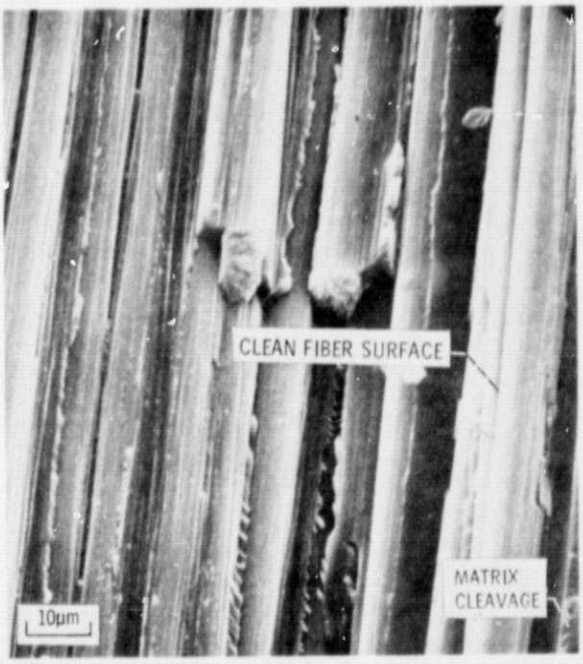

(c) ENLARGEMENT OF DETAIL IN (b) TO SHOW FRACTURE MODE.

Figure 13. - Scanning electron photomicrographs of fractured surface of MOD I/Epoxy composite $[0]_8$ tested at 75 degrees to the fiber direction.

(a) GENERAL VIEW

(b) DETAILED VIEW

(c) ENLARGEMENT OF DETAIL IN (b) TO SHOW FRACTURE MODE.

Figure 14. - Scanning electron photomicrographs of fractured surface of MOD I/Epoxy composite $[0]_8$ tested transverse to the fiber direction.